Amide proton signals as pH indicator for *in vivo* MRS and MRI of the brain—Responses to hypercapnia and hypothermia

Takashi Watanabe *, Jens Frahm, Thomas Michaelis

Biomedizinische NMR Forschungs GmbH am Max-Planck-Institut für biophysikalische Chemie, Göttingen, Germany

A B S T R A C T

Using proton MRS and MRI of mouse brain at 9.4 T, this work provides the first *in vivo* evidence of pH-dependent concurrent changes of three amide signals and related metabolic responses to hypercapnia and hypothermia. During hypercapnia, amide proton MRS signals of glutamine at 6.8–6.9 ppm and 7.6 ppm as well as of unspecific compounds at 8.1–8.3 ppm increase by at least 50% both at 37 °C and 22 °C. These changes reflect a reduced proton exchange with water. They are strongly correlated with intracellular pH which ranges from 6.75 ± 0.10 to 7.13 ± 0.06 as determined from a shift in creatine phosphokinase equilibrium. In MRI, saturation transfer from aliphatic as well as from aromatic and/or amide protons alters slightly during hypercapnia and significantly during hypothermia. The asymmetry in magnetization transfer ratios decreased slightly during hypercapnia and hypothermia. Regardless of pH or temperature, saturation transfer from aliphatic protons between -2 and -4 ppm frequency offset to water protons is significantly greater than that from aromatic/amide protons at corresponding offsets between $+2$ and $+4$ ppm. Irradiation of aliphatic compounds at -3.5 ppm frequency offset from water predominantly saturates lipids and water associated with myelin. Taken together, the results indicate that, for the B_1 power used in this study, dipolar coupling between aliphatic and water protons rather than proton exchange is the dominant factor in Z-spectra and magnetization transfer ratio asymmetry of the brain *in vivo*.

© 2016 Elsevier Inc. All rights reserved.

Introduction

Magnetic resonance (MR) spectroscopy (MRS) and imaging (MRI) play important roles in translational biomedical research and in particular allow for a biochemical phenotyping of the brain. Complementing the neurochemical profiling by *in vivo* MRS, there have been manifold investigations of pH dependencies, mainly with the use of ^{31}P MRS. Exploiting the higher sensitivity of ^1H MRS at 4.7 T, amide signals in brain spectra were found to change with pH, because they exchange protons with water in base-catalyzed reactions (Kanamori and Ross, 1997; Mori et al., 1998; Zhou and van Zijl, 2006). While two amide resonances of glutamine (Gln) at 6.8–7.6 ppm were studied by nuclear

Overhauser enhancement (NOE) through ^{15}N excitation after administration of exogenous $^{15}NH_4^+$ (Kanamori and Ross, 1997), amide signals of proteins and peptides around 8.3 ppm were identified by MRS sequences with minimized saturation transfer from water (Mori et al., 1998; Zhou and van Zijl, 2006).These base-catalyzed exchange reactions are also responsible for the contrast described in chemical exchange saturation transfer (CEST) MRI (Zhou and van Zijl, 2006).

Here, we report saturation transfer MRS and MRI studies of proton exchange in mouse brain *in vivo* at 9.4 T, which detect all aforementioned amide protons without the use of $^{15}NH_4^+$ or the need for special pulse sequences. At a high field of 9.4 T, the application of a common MRS technique with effective water pre-saturation yields a significant increase of amide signals, i.e., reduced amide–water proton exchange, in response to hypercapnia and hypothermia.
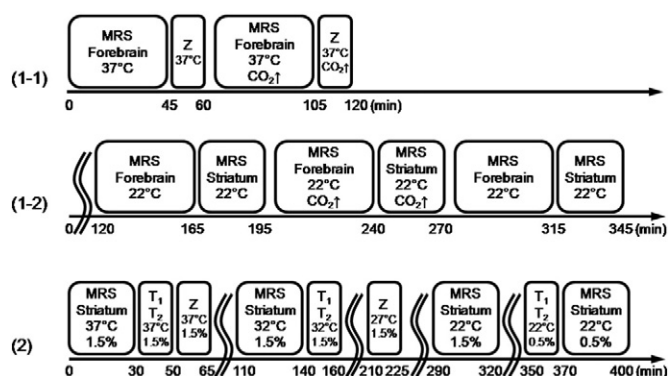
Materials and methods

Animals and anesthesia

A total of 11 female C57BL/6N mice (4–5 months, 23–29 g) were studied in accordance with German animal protection laws after approval by the responsible governmental authority. As shown in Fig. 1, 5 mice underwent MRS of the forebrain and acquisition of the Z-spectra before and during hypercapnia at 37 °C (protocol 1-1)

Fig. 1. Time course of three MRS and MRI protocols (Z-spectrum, T_1 and T_2 relaxation times) for two animal groups measured with or without hypercapnia ($CO_2\uparrow$) at different temperatures under 1.5% or 0.5% isoflurane anesthesia. Z = Z-spectrum. For details, see text.

followed by MRS of the forebrain and of the striatum before, during, and after hypercapnia at 22 °C one day later (protocols 1–2). Another 6 mice underwent MRS of the striatum, T_1, T_2, and/or Z-spectra measurements of the striatum at 37 °C ($n = 6$), 32 °C ($n = 4$), 27 °C ($n = 5$), and/or 22 °C ($n = 5$) under 1.5 or 0.5% isoflurane anesthesia (protocol 2). After induction of anesthesia with 5% isoflurane, animals were intubated with a purpose-built polyethylene endotracheal tube (0.58 mm inner diameter, 0.96 mm outer diameter) and artificially ventilated using an animal respirator (TSE, Bad Homberg, Germany) with a respiratory rate of 25 breaths per minute and an estimated tidal volume of 0.35 ml as previously described (Schulz et al., 2002; Watanabe et al., 2004; Boretius et al., 2013). The animals were then placed in a prone position on a purpose-built palate holder equipped with an adjustable nose cone. The Göttingen animal bed (Tammer et al., 2007) secured a reproducible and reliable fixation of the mouse head and receiver coil in the magnet isocenter. Respiratory movement of the abdomen as well as rectal temperature were monitored by a unit supplied by the manufacturer (Bruker Biospin MRI GmbH, Ettlingen, Germany). Thirty minutes after the rectal temperature reached 37 ± 1 °C, 32 ± 1 °C, 27 ± 1 °C, or 22 ± 1 °C with the use of a heating system (i.e., a water blanket and animal bed), the respective chemical shifts of the N-acetylaspartate (NAA) amide signal at 7.83–7.84, 7.87–7.88, 7.91–7.92, and 7.95–7.96 ppm confirmed the brain temperature to be within the target range (Arús et al., 1985). MRS and MRI data were acquired only after the equilibrium was established.

MRS

At 9.4 T (Bruker Biospin MRI GmbH, Ettlingen, Germany), localized proton MRS (STEAM, TR/TE/TM = 6000/10/10 ms) was performed with the use of a birdcage resonator (inner diameter 70 mm) and a saddle-shaped quadrature surface coil (both Bruker Biospin MRI GmbH, Ettlingen, Germany) on anesthetized mice as previously described (Boretius et al., 2013). A $(40\ mm)^3$ cubic volume-of-interest was centered on the forebrain or a $(20\ mm)^3$ volume-of-interest on the right striatum (Boretius et al., 2013). Water saturation was accomplished by means of three Gaussian-shaped CHESS radiofrequency (RF) pulses (90°–90°–180°), each of which with a duration of 7.83 ms and a bandwidth of 350 Hz. The overall duration of the CHESS module was 147 ms. Each CHESS pulse was followed by an associated spoiler gradient and a 37 ms outer volume saturation module covering a range of 3 mm around the volume-of-interest without gap.

Metabolite quantification involved spectral evaluation by LCModel (Provencher, 1993) and calibration with brain water concentration of 79% (Duarte et al., 2014), for which the unsuppressed water proton signal served as internal reference. Amide signal intensities of different compounds were normalized to and expressed as those of NAA in

each spectrum. Intraindividual variations in NAA amide signal intensities during hypercapnia were corrected for variations in concentration by normalization with NAA as determined by LCModel. With TE = 10 ms, the unsuppressed water signal was assumed to be attenuated by 22% between the temperatures at 37 °C and 22 °C, because T_2 relaxation times of water protons in the $(20\ mm)^3$ volume-of-interest were determined by a multi-echo spin-echo MRI (TR/TE = 2500/10–123 ms) to be 41.0 ± 0.6 ms at 37 °C and 40.0 ± 1.5 ms at 22 °C ($n = 5$). T_1 relaxation times were determined with the use of a spin-echo saturation recovery sequence and 7 TR values from 0.15 to 6 s. Metabolites with Cramer–Rao lower bounds above 20% were excluded from further analysis. Significant differences between two groups of data were determined by a Student's two-sided t-test as well as by the Wilcoxon's signed rank (for paired comparisons) or rank sum (for unpaired comparisons) test. p values for the non-parametric tests are given as p'. The standard general linear model was fitted to examine a linear relationship between two variables because the animal effects did not account for a meaningful amount of variance in the random effects when the linear mixed-effects model was fitted (SPSS® version 21.0, IBM®).

In addition, for validating the source of observed MRS signals at 6.81–6.9 ppm and 7.6 ppm in brain *in vivo* as Gln as well as their dependence on pH, 10–100 mM Gln, Cr, or PCr (SERVA Feinbiochemica, Heidelberg, or Sigma-Aldrich Chemie, Taufkirchen, Germany) in 0.2 M sodium phosphate buffer with pH 6.2–7.4 was measured using localized MRS (STEAM, TR/TE/TM = 10,000–15,000/10/10 ms) at 16–37 °C.

pH estimation

Intracellular pH in brain tissue was estimated from the creatine phosphokinase equilibrium: $ATP + Cr \leftrightarrow ADP + PCr + H^+$ yielding $[H^+] = ([ATP] \times [Cr] \times K')/([ADP] \times [PCr])$. [ATP]/[ADP] is calculated to 11.47 with the equilibrium constant $K' = 7.09 \times 10^{-9}$ at 37 °C taken from the literature (Siesjö et al., 1972; Kass and Lipton, 1982; Whittingham et al., 1984). For the exothermic reaction, K' is corrected with $\Delta H = -1550$ cal/mol (Noda et al., 1954; Ohlmeyer, 1946) according to the van't Hoff equation yielding $K' = 7.39 \times 10^{-9}$ at 32 °C and 8.06×10^{-9} at 22 °C. The tissue concentrations of ATP and ADP are known to be unaffected by the type of anesthesia, hypercapnia, or hypothermia (Folbergrová et al., 1972; Hägerdal et al., 1975; Nilsson and Siesjö, 1974; Siesjö et al., 1972).

MRI

For both MRI and MRS, shimming of the B_0 field was carried out by FASTMAP (Gruetter, 1993). For measurements of S_{sat}/S_0, i.e., Z-spectrum (Zhou and van Zijl, 2006), an off-resonance Gaussian-shaped RF pulse with a duration of 12 ms and a flip angle of 180° (2.3 μT) was incorporated into a spin density-weighted gradient-echo MRI sequence (RF-spoiled 3D FLASH, TR/TE = 24/4.5 ms, flip angle 5°, field-of-view $(16\ mm)^3$, matrix $64 \times 64 \times 32$, measuring time 48 s, duty cycle 50%) at a resolution of $250 \times 250 \times 500$ μm³ (Supplementary Fig. 1). The duration and power of the off-resonance pulse was optimized to observe the transfer of saturation from non-water protons to water protons in brain of mice *in vivo* (Natt et al., 2003; Watanabe et al., 2012). A stronger off-resonance irradiation, in particular at small frequency offset, would unfavorably increase a direct saturation of water protons and therefore was not used. High-resolution MTR maps were obtained from acquisitions with and without off-resonance irradiation at a resolution of $120^2 \times 600$ μm³ (TR/TE = 30/7.6 ms, flip angle 5°, field-of-view $15.4 \times 15.4 \times 19.2$ mm³, matrix $128 \times 128 \times 32$, measuring time 8 min, $n = 3$). For the evaluation of MRI signal intensities, square-shaped regions of interest with 36 pixels were selected in the striatum (Supplementary Fig. 1) in a standardized manner. The analysis followed a strategy previously developed for intraindividual comparisons of MR images obtained after manganese administration (Watanabe et al., 2004).

Results

MRS

As shown in Fig. 2a and Supplementary Fig. 2, cerebral lactate (Lac) in the forebrain was strongly elevated at 37 °C under 1.5% isoflurane anesthesia. Halogenated volatile anesthetics inhibit the cellular respiration (Rosenberg and Haugaard, 1973; Boretius et al., 2013), which in turn accelerates anaerobic glycolysis to meet the energy demand. In the aromatic range, proton signals from urea (5.75 ppm) and amides of Gln H_Z (6.81 ppm) and NAA (7.83 ppm) are readily resolved as well as aromatic hydrocarbons of histidine/homocarnosine (7.09 ppm) and tryptophan/ phenylalanine (7.26 ppm) (Vermathen et al., 2000). With 4 protons per molecule, urea provides high signal intensities in line with the reported
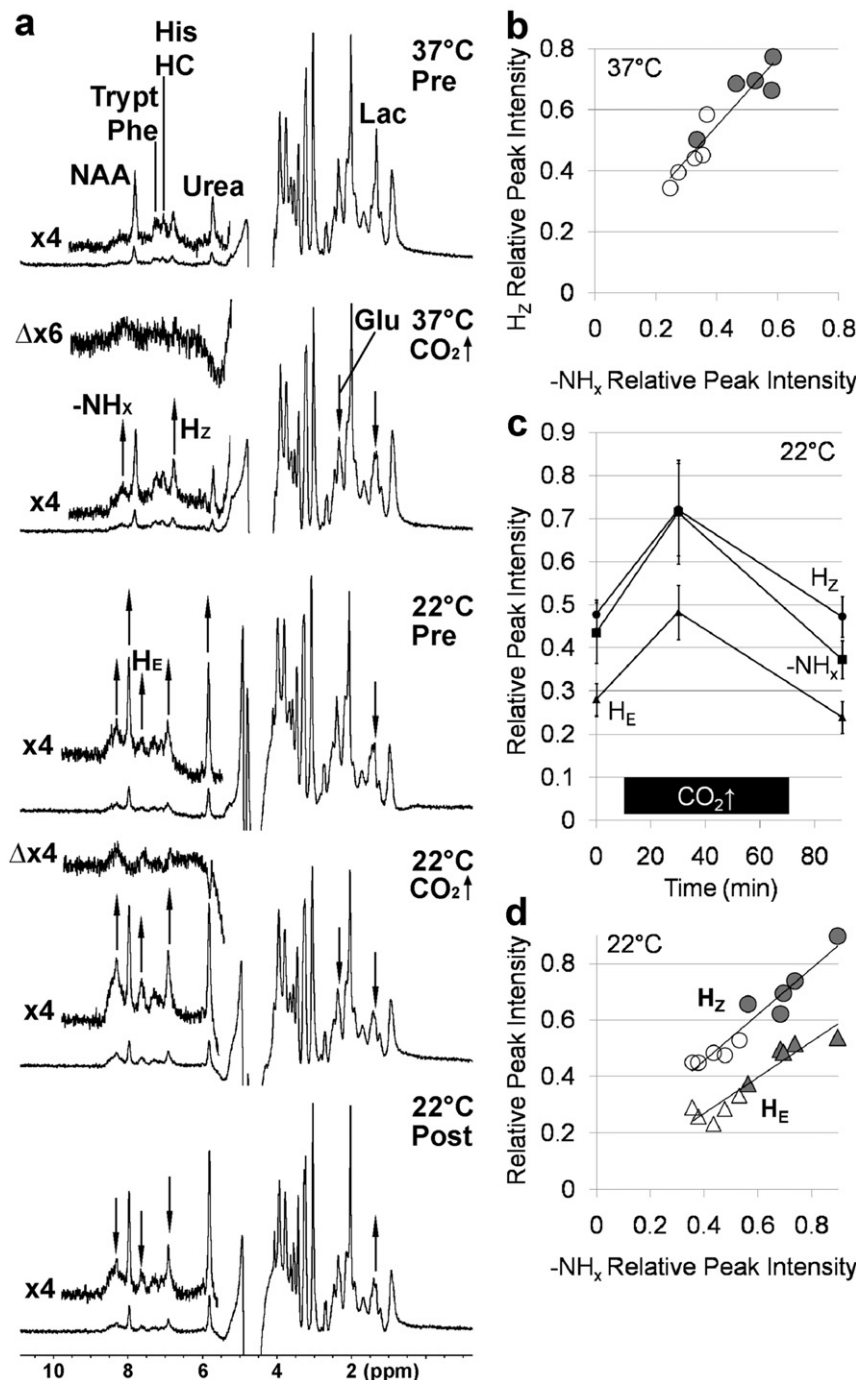
Fig. 2. MRS signal changes during hypercapnia and hypothermia. (a) (37 °C, Pre) MRS before as well as (37 °C, CO₂↑) during hypercapnia at 37 °C, and (22 °C, Pre) MRS before, (22 °C, CO₂↑) during as well as (22 °C, Post) after hypercapnia at 22 °C: STEAM, TR/TE/TM = 6000/10/10 ms, 384 averages, (4 mm)³ localized in the forebrain of mice *in vivo*, processed with a 1-Hz line broadening, averaged across 5 animals. Glu = methylene bridge protons of glutamate, HC = homocarnosine, His = histidine, H_E and H_Z = amide protons of glutamine, Lac = lactate, NAA = N-acetylaspartate, -NH_X = unspecific amide protons, Phe = phenylalanine, Trypt = tryptophan, ×4 = magnified, Δ = difference between Pre and CO₂↑, ↑ = significant signal intensity increases, ↓ = significant signal intensity decreases. (b) Relative signal intensities of H_Z amide protons of glutamine plotted versus those of unspecific amide protons -NH_X taken from 5 animals (empty circles) before and (filled circles) during hypercapnia at 37 °C (cf., top and second rows in Fig. 2a.) $y = 1.1x + 0.1$, $r = 0.94$, $p = 1.8E-07$. (c) Relative signal intensities (mean ± SD, $n = 5$) of H_E, H_Z and -NH_X amide protons before, during, and after hypercapnia at 22 °C (cf., third, fourth, and fifth rows in Fig. 2a) plotted over time. (d) Relative signal intensities of H_Z ($y = 0.82x + 0.13$, $r = 0.96$, $p = 7.8E-09$), H_E ($y = 0.63x - 0.02$, $r = 0.94$, $p = 1.3E-07$), and -NH_X amide protons taken from 5 animals (empty markers) before and (filled markers) during hypercapnia at 22 °C (cf., third and fourth rows in Fig. 2a).
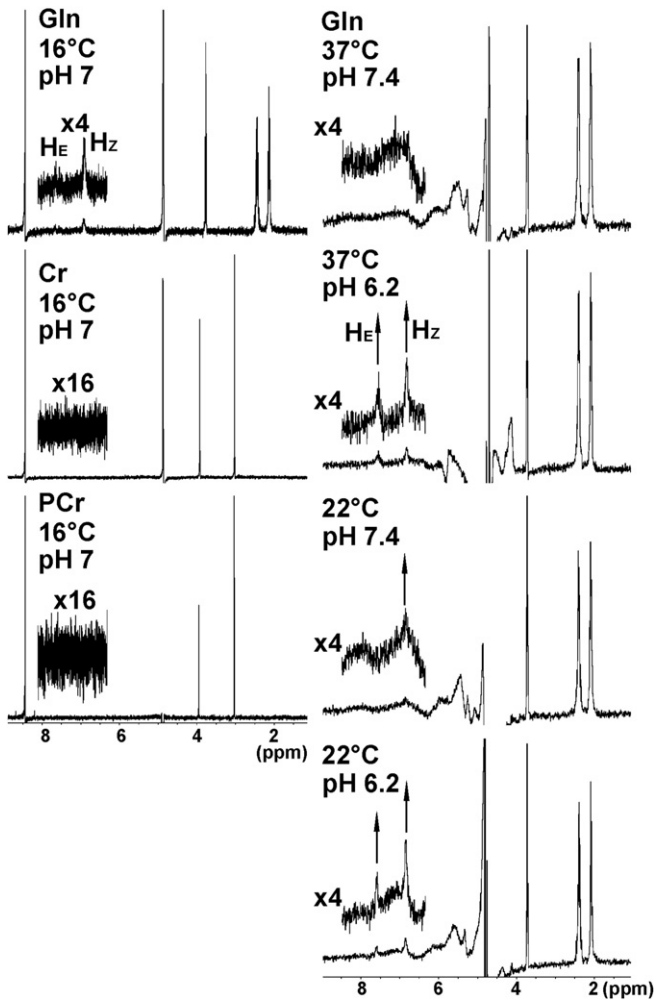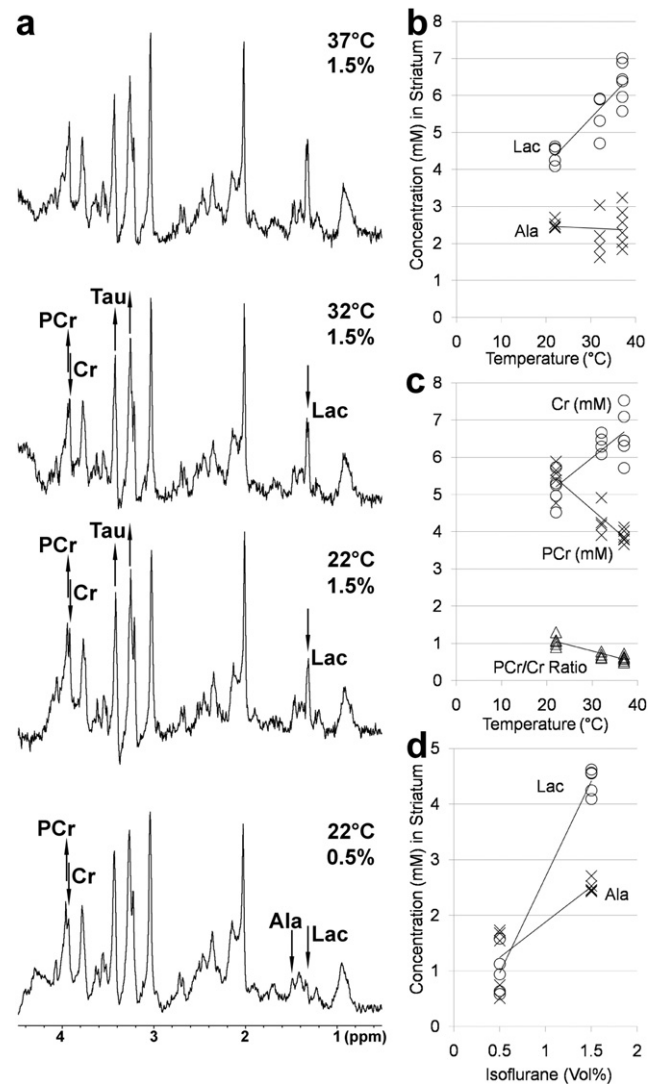
Fig. 3. (Left) (Gln) Proton resonances at 2.10–2.13, 2.43–2.46, 3.75, 6.8–6.9, and 7.5–7.6 ppm acquired from 100 mM aqueous solution of glutamine, (Cr) at 3.03 and 3.91 ppm acquired from 50 mM aqueous solution of creatine, and (PCr) at 3.03 and 3.93 ppm acquired from 25 mM aqueous solution of phosphocreatine at 16 °C with pH 7, respectively. The formic acid is used as a reference that yields a resonance at 8.46 ppm. STEAM localization, TR/TE/TM = 15,000/10/10 ms, 128 averages, (4 mm)^3, H_E and H_Z = amide protons of glutamine, ×4 and ×16 = magnified. (Right) Proton resonances acquired from 10 mM aqueous solution of glutamine at 37 °C and 22 °C with pH 7.4 and pH 6.2, respectively. TR/TE/TM = 10,000/10/10 ms, 32 averages, (8 mm)^3, 1-Hz line broadening.

Fig. 4. Effect of hypothermia and isoflurane reduction on metabolite concentrations in the striatum *in vivo*. (a) MRS (256 averages, (2 mm)^3, for other parameters see Fig. 2a) at 37 °C, 32 °C, or 22 °C with 1.5 or 0.5 Vol% isoflurane concentration. Ala = alanine, Cr = creatine, PCr = phosphocreatine, Tau = taurine. For other abbreviations, see the legend of Fig. 2a. (b, c) Lactate ($y = 0.13x + 1.5$, $r = 0.88$, $p = 1.2E-05$), alanine ($y = -0.005x + 2.6$, $r = -0.08$, $p = 0.78$), phosphocreatine ($y = -0.11x + 7.8$, $r = -0.91$, $p = 2.2E-06$), and creatine ($y = 0.097x + 3.1$, $r = 0.81$, $p < 0.001$) concentrations as well as the ratio of the concentration of phosphocreatine to that of creatine ($y = -0.032x + 1.8$, $r = -0.90$, $p = 6.6E-06$) in the striatum taken from 5 animals plotted versus temperature (cf., top, second, and third rows in Fig. 4a). (d) Lactate ($y = 3.4x - 0.75$, $r = 0.99$, $p = 2.0E-11$) and alanine ($y = 1.3x + 0.61$, $r = 0.87$, $p = 3.1E-05$) concentrations taken from 5 animals plotted versus Vol% isoflurane concentration (cf., third and fourth rows in Fig. 4a).

concentration of 2.6–2.9 mmol/kg wet weight in brain (Moats et al., 1993).

The addition of 15% CO_2 to the inspiratory gas (1.5% isoflurane in 30% O_2) significantly ($p < .01$, $p' < .05$) lowered the concentration of Lac (normalized to total creatine (tCr)) within 30 min to an undetectable level, and that of glutamate (Glu) by 19% ($p < .01$, $p' < .05$). These findings indicate that (i) the CO_2-induced pH reduction inhibits the anaerobic glycolysis (Yudkoff et al., 2000) and (ii) Glu substitutes glucose (Glc) as a metabolic fuel to maintain energy support (Erecińska et al., 1988). In the aromatic range, CO_2 increased the amide intensity of Gln H_Z (relative to NAA amide) from 0.44 ± 0.09 by 50% to 0.66 ± 0.1 ($p < .01$, $p' < .05$) and that of unspecific origin (-NH$_X$: 8.16 ppm) from 0.31 ± 0.05 by 59% to 0.50 ± 0.1 ($p < .05$, $p' = .05$). This alteration results from a reduced proton exchange with water. The relative resonance intensities of H_Z and -NH$_X$ are strongly correlated with each other (Fig. 2b). The intensities of the urea resonance did not alter during hypercapnia.

At 22 °C, the isoflurane level necessary for anesthesia may be reduced to 0.5%, which reduces Lac accordingly (Fig. 2a). In the aromatic range, the signals of urea (5.8 ppm), Gln amide (H_Z: 6.9 ppm), NAA

amide (7.95 ppm), and unspecific amides (-NH$_X$: 8.28 ppm) increased in response to hypothermia, which again may be explained by reduced proton exchange with water. Under these conditions, a further amide signal of Gln (H_E: 7.6 ppm) could be identified. The addition of 15% CO_2 to the inspiratory gas (0.5% isoflurane in 30% O_2) increased the relative intensities of H_Z, H_E, and -NH$_X$, from 0.48 ± 0.03, 0.28 ± 0.04, and 0.43 ± 0.07 by 51%, 72%, and 64% to 0.72 ± 0.11, 0.48 ± 0.06, and 0.71 ± 0.12 ($p < .01$ and $p' < .05$ for each), respectively. Conversely, the interruption of CO_2 reduced these values to 0.47 ± 0.05, 0.24 ± 0.04, and 0.37 ± 0.04 ($p < .01$, <.001, and <.001; $p' < .05$ for each) (Fig. 2c). Lac and Glu changes are in line with the behaviour seen at 37 °C. The relative intensities of H_Z and -NH$_X$ as well as of H_E and -NH$_X$ are strongly correlated with each other (Fig. 2d). The source of the H_Z and H_E signals as well as their dependence on pH was validated
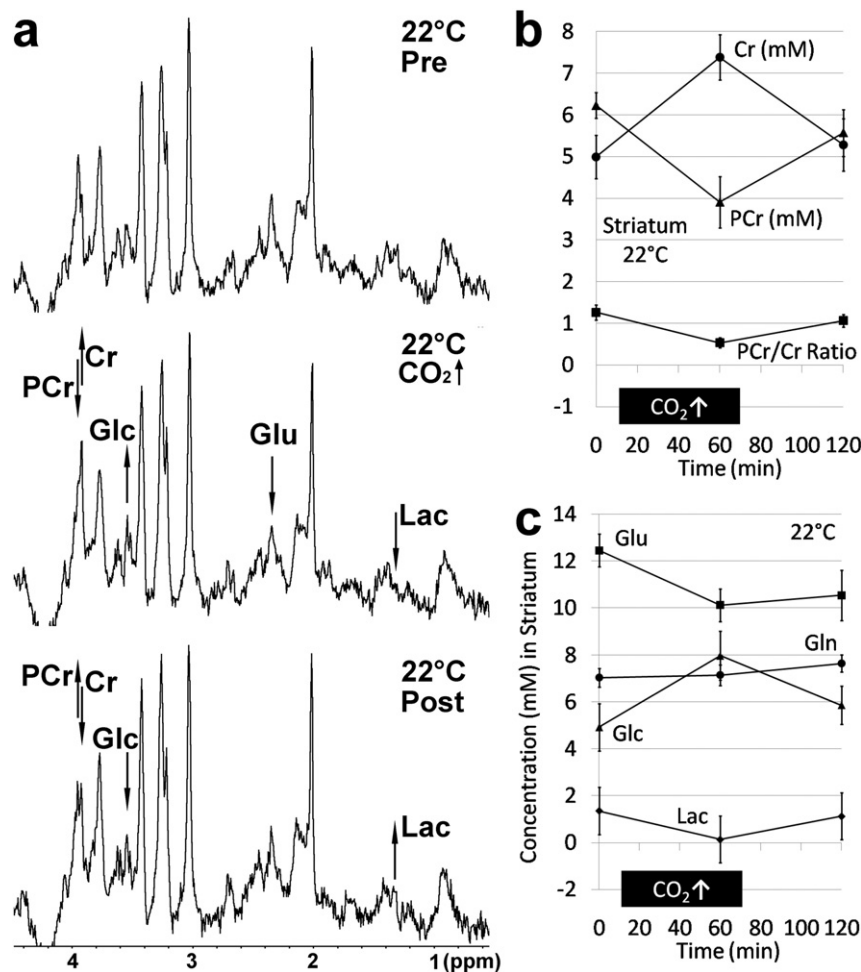
Fig. 5. Effect of hypercapnia on metabolite concentrations in the striatum *in vivo* at 22 °C. (a) (22 °C, Pre) MRS (for parameters see Fig. 4a) before, (22 °C, CO₂↑) during, or (22 °C, Post) after hypercapnia. Glc = glucose. For other abbreviations, see the legends of Figs. 2a and 4a. (b) Phosphocreatine and creatine concentrations as well as the ratio of their concentrations plotted versus time (mean ± SD, $n = 5$). (c) Glutamate, glutamine (Gln), glucose, and lactate concentrations plotted versus time (mean ± SD, $n = 5$).
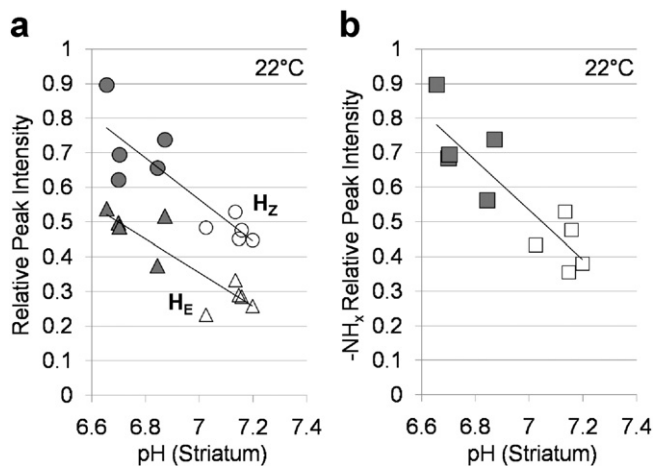

Fig. 6. Correlations between MRS amide proton signal intensities and pH. (a) Relative signal intensities of H_Z ($y = -0.60x + 4.8$, $r = -0.87$, $p = 3.1E-05$), H_E ($y = -0.49x + 3.8$, $r = -0.88$, $p = 1.3E-05$), and (b) -NH_X ($y = -0.72x + 5.6$, $r = -0.88$, $p = 1.9E-05$) amide protons taken from 5 animals (empty markers) before and (filled markers) during hypercapnia at 22 °C (cf., third and fourth rows in Fig. 2a, Fig. 2d) plotted versus brain pH estimated from the ratio of the concentrations of phosphocreatine/creatine (cf. Fig. 5b).

in vitro as shown in Fig. 3. They can be neither of Cr nor of PCr. Even when the rate of proton exchange is reduced (16 °C), they yield no observable signal in the aromatic range at around physiological pH. It is also of note that an acquisition without water suppression revealed 7.0 ± 2.7% larger water resonance areas *in vivo* at 22 °C than at 37 °C ($n = 4$). This physical effect corresponds to the more favorable Boltzmann distribution of proton spins at lower temperatures.

Metabolite concentrations

In the striatum, as shown in Figs. 4a, b, hypothermia reduced Lac most significantly. The absence of a concomitant alanine decrease suggests that (i) the productions of pyruvate and Lac were equally reduced due to a lower energy consumption/demand, while (ii) cellular respiration remained impaired by isoflurane. Further, hypothermia decreased creatine (Cr) and increased phosphocreatine (PCr) (Figs. 4a, c). This is because a reduced energy consumption increases intracellular pH, which was estimated to be 6.86 ± 0.06 at 37 °C, 6.90 ± 0.05 at 32 °C, and 7.06 ± 0.06 at 22 °C. During hypothermia taurine (Tau) signals increased at 32 °C ($p < .05$, $p' < .05$) and 22 °C ($p < .01$, $p' < .01$). However, the effect is due to the long proton T_1 of 2.6 s at 37 °C and 9.4 T (Cudalbu et al., 2009), so that after correcting for T_1 saturation (i.e., after multiplication by $(1-e^{-TR/T1})$), the Tau concentration turned out to be unaffected by hypothermia. This interpretation was further supported by the observation of a Tau signal increase at 37 °C when TR was prolonged to 10 s. At 22 °C, the reduction of the isoflurane administration from 1.5%
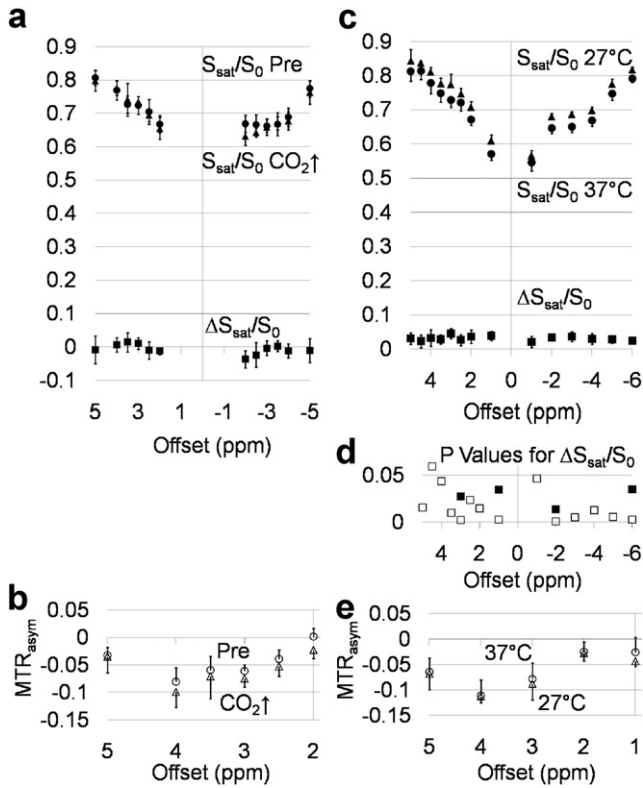
Fig. 7. MRI S_{sat}/S_0 spectrum changes during hypercapnia and hypothermia. (a) (S_{sat}/S_0 Pre, filled circles) Spectrum before and (S_{sat}/S_0 $CO_2\uparrow$, filled triangles) during hypercapnia and ($\Delta S_{sat}/S_0$) their differences. (b) (Pre, empty circles) MTR_{asym} spectrum before and ($CO_2\uparrow$, empty triangles) during hypercapnia. (c) S_{sat}/S_0 spectrum at 37 °C or 27 °C and (Δ) their differences. (d) (Empty squares) p values of Student's paired t-test for differences between S_{sat}/S_0 at 37 °C and 27 °C without and (filled squares) with Bonferroni correction for the multiple comparison: $p < .05$ at 3.0, 1.0, −2.0, and −6.0 ppm. (e) MTR_{asym} spectrum at (empty circles) 37 °C or (empty triangles) 27 °C.

Fig. 8. MTR maps showing magnetization transfer from (−3.5 ppm (H_2O)) aliphatic and (+3.5 ppm (H_2O)) aromatic/amide compounds. Radiofrequency-spoiled 3D FLASH (TR/TE = 30/7.6 ms, flip angle 5°, off-resonance pulse 180°/12 ms, resolution $120^2 \times 600$ μm³, measuring time 8 min) of mouse brain *in vivo* in mid-sagittal sections. White arrows = the fornix, anterior commissure, corpus callosum and cerebellar white matter (from left to right).

to 0.5% markedly reduced Lac and also decreased alanine (Fig. 4d). This suggests that (i) the production of pyruvate was reduced to a greater degree than that of Lac, while (ii) the cellular respiration was largely restored. For the same amount of energy, oxidative phosphorylation requires less pyruvate than anaerobic glycolysis. As a result of reduced glycolysis and acid production, the pH increased slightly to 7.09 ± 0.07.

At 22 °C (Fig. 5a), the addition of 15% CO_2 to the inspiratory gas (0.5% isoflurane in 30% O_2) increased Cr from 5.0 ± 0.5 to 7.4 ± 0.5 mM ($p < .001$, $p' < .05$) and decreased PCr from 6.2 ± 0.3 to 3.9 ± 0.6 mM ($p < .001$, $p' < .05$) (Fig. 5b). The corresponding pH reduced from 7.13 ± 0.06 to 6.75 ± 0.10 ($p < .001$, $p' < .05$). On the other hand, the interruption of CO_2 decreased Cr to 5.3 ± 0.6 mM ($p < .01$, $p' < .05$) and increased PCr to 5.6 ± 0.6 mM ($p < .001$, $p' < .05$), while the pH increased to 7.06 ± 0.06 ($p < .01$, $p' < .05$). Glc changed from 4.9 ± 1.0 to 8.0 ± 1.0 ($p < .01$, $p' < .05$) and then to 5.9 ± 0.8 mM ($p < .05$, $p' < .05$), while Lac changed from 1.4 ± 0.6 to 0.13 ± 0.2 ($p < .05$, $p' < .05$) and back to 1.1 ± 0.3 mM ($p < .01$, $p' < .05$) (Fig. 5c) because pH reduction inhibits glycolysis (Yudkoff et al., 2000). Glu, which substitutes Glc as a metabolic fuel (Erecińska et al., 1988), decreased from 12.5 ± 0.7 to 10.1 ± 0.7 mM ($p < .01$, $p' < .05$) in line with the observation in Fig. 2a. After the interruption of CO_2, Glu did not recover to basal values (10.6 ± 1.1, $p < .01$ and $p' < .05$ vs. pre), confirming that Glu reduction during hypercapnia does not result from a simple pH-dependent equilibrium shift, but from its metabolic consumption as a fuel. Gln increased during and after hypercapnia slightly ($p = 0.5$ and 0.10; $p' = 0.2$ and 0.04), which suggests accelerated systemic ammonia production and its subsequent incorporation into brain Gln (Kazemi

and Johnson, 1986). The relative intensities of H_Z, H_E, and $-NH_X$ were significantly correlated with pH (Figs. 6a, b).

MRI

Fig. 7a shows that hypercapnia slightly altered the Z-spectrum. Between 3 and 4 ppm (offset from water proton resonance frequency; H_2O), where the amide protons of unspecific origin ($-NH_X$) are supposed to be saturated most effectively, CO_2 reduced the magnetization transfer ratio (MTR) by 0.01 ± 0.02. Accordingly, the asymmetry in MTR (MTR_{asym}) (Zhou and van Zijl, 2006) (Fig. 7b) decreased during hypercapnia by 0.014 ± 0.007 (averaged across 2–5 ppm (H_2O), not significant), i.e., on average ($n = 5$) from 0.002, -0.04, -0.06, -0.06, -0.08, and -0.032 (Pre) to -0.02, -0.05, -0.08, -0.07, -0.10, and -0.035 ($CO_2\uparrow$) at 2, 2.5, 3, 3.5, 4, and 5 ppm (H_2O), respectively, with the largest drop by 0.02 at 2 ppm (H_2O). This MTR reduction in the aromatic range during hypercapnia was most likely caused by reduced chemical exchange between amide and water protons (Zhou et al., 2003; Zhou and van Zijl, 2006).

Figs. 7c, d show that a 10° temperature reduction lowered the off-resonance saturation (except at +4.5 ppm (H_2O)). The MTR decreased in the aromatic range, averaged across 1 to 5 ppm (H_2O), by 0.032 ± 0.02 and in the aliphatic range, averaged across −1 to −5 ppm (H_2O), by 0.030 ± 0.01. Thus, MTR_{asym} (Fig. 7e) shows a slight (not significant) drop (by 0.007 ± 0.02 averaged across 1–5 ppm (H_2O)) upon hypothermia, i.e., from mean values of -0.025, -0.025, -0.079, -0.111, and -0.065 (37 °C) to -0.043, -0.028, -0.088, -0.113, and -0.068 (27 °C) at 1, 2, 3, 4, and 5 ppm (H_2O), respectively, with the largest decrease at 1.0 ppm. In other words, MTR increases upon temperature rise more in the aromatic than in the aliphatic range. This can be ascribed to increased proton exchange (e.g., $0.007/0.032 = 22\%$) and smaller relaxation rates R_1 (e.g., 78%) of water protons. R_1 in the striatum can be calculated to be 0.61 s^{-1} at 37 °C and 0.69 s^{-1} at 27 °C (Supplementary Fig. 3). T_1 relaxation times were shortened

from 1.67 ± 0.06 s at 37 °C to 1.48 ± 0.04 s at 32 °C and 1.38 ± 0.08 s at 22 °C.

Figs. 7a, b, c, e also show that S_{sat}/S_0 is constantly higher in the aromatic range, i.e., MTR_{asym} is negative. At 2.5, 3, 3.5, and 4 ppm (H_2O), S_{sat}/S_0 is significantly higher than at -2.5, -3, -3.5, and -4 ppm (H_2O), respectively, before ($p < .01$, $<.001$, $<.01$, and $<.01$; $p' < .05$ for each) and during ($p < .01$, $<.001$, $<.05$, and $<.01$; $p' < .05$ for each) hypercapnia. S_{sat}/S_0 is also significantly higher at 2, 3, 4, and 5 ppm (H_2O) than at -2, -3, -4, and -5 ppm (H_2O), respectively, before ($p < .05$, $<.01$, $<.01$, and $<.01$ or $p' < .05$ for each) and during ($p < .05$, $<.01$, $<.001$, and $<.01$ or $p' < .05$ for each) hypothermia. This indicates that non-water protons in the brain *in vivo* are largely those of aliphatic compounds between -3.9 and -0.1 ppm (H_2O), e.g., methyl (CH_3-) and methylene bridge (-CH_2-) protons. Accordingly, as shown in Fig. 8, irradiation at -3.5 ppm (H_2O) frequency offset saturates the water signal of the myelinated structures, rich in lipids and proteolipids, more than irradiation at $+3.5$ ppm (H_2O). For example, the MTR in the corpus callosum is 0.44 ± 0.01 for -3.5 ppm irradiation as opposed to 0.26 ± 0.04 ($n = 3$, $p < .05$, $p' = 0.11$). Moreover, the -3.5 ppm (H_2O) irradiation results in a greater white/gray matter contrast yielding $MTR = 0.27 \pm 0.05$ in the cerebral cortex versus 0.44 ± 0.01 ($p < .05$, $p' = 0.11$), whereas the $+3.5$ ppm (H_2O) irradiation of aromatic compounds and amide protons provides only a weak difference in the cerebral cortex with $MTR = 0.24 \pm 0.05$ compared to 0.26 ± 0.04. This observation is in agreement with the fact that neither the protein content (except proteolipids: about 10–11%) nor the nucleic acid content (about 0.14%) is significantly different between white and gray matter (Clausen, 1969; Norton, 1975). In other words, the relative contribution of proteins and nucleic acids (among all kinds of macromolecules) on MTR is so much larger in gray than in white matter as the semisolid macromolecules of myelin lipids are less concentrated in gray matter (i.e., the contribution from lipids is smaller in gray than in white matter).

Discussion

The present study at a high magnetic field not only confirms earlier MRS observations of 8.3 ppm proton signals (Mori et al., 1998) and more recent CEST MRI findings (Zhou and van Zijl, 2006), but clearly demonstrates that the 8.3 ppm signal intensities strongly correlate with both amide signals of Gln as well as with pH. It is shown for the first time that the three peaks concurrently change as a function of pH. In previous work (Mori et al., 1998), only one peak around 8.3 ppm was detected and "tentatively assigned" to nucleosides and proteins. The present study demonstrates that this resonance most likely stems from exchanging amide protons. Its intensity strongly correlates with those of exchanging amide protons of Gln. The sources of the resonances at 6.81–6.9 ppm and 7.53–7.6 ppm as well as their pH-dependence at 22–37 °C in brain *in vivo* was validated with Gln solution *in vitro*, which also confirms the results acquired from ^{15}N-glutamine solution by ^{15}N excitation (Kanamori and Ross, 1997). The lack of detectable resonances from Cr and PCr in the aromatic range around physiological pH (Fig. 3) is in line with a previous observation (Haris et al., 2012). It suggests that effects of Gln amides around ~2.1 and ~2.8 ppm (H_2O) could hardly be distinguished from (or could be dominated by) those of Cr or PCr amines (or amides) around ~1.9 or ~2.6 ppm (H_2O) in Z-spectra. Given that the amide signal changes can be observed by commonly available proton MRS sequences and that CEST MRI finds increasing applications, it is foreseeable that MRS of amide–water proton exchange as well as CEST MRI will lead to new research applications of preclinical and clinical interest. It remains to be elucidated and may depend on the scientific question whether the low spatial resolution of MRS is a relevant disadvantage compared to CEST MRI when considering its specificity and sensitivity for detecting changes in pH, temperature, or concentration of many metabolites in brain *in vivo*.

The amide–water proton exchange in brain *in vivo* is more specifically observable by MRS than by Z-spectra or MTR_{asym}. This is because of two reasons: First, a number of short-T_2 protons around 6.8–8.3 ppm do not interfere with these resonances and, second, water protons can much more effectively be saturated than amide protons. In MRS, a chemical-shift selective irradiation readily saturates at least 99.9% of the protons of water (Frahm et al., 1990) that makes up ~82% of the brain *in vivo* in wet weight. The signal intensities of Gln H_Z, Gln H_E, and unspecific amides -NH_X are a direct measure of water-amide proton exchange rate because the degree of saturation of water protons as well as the spin density of amide protons is unaffected by exchange rate. Moreover, the MRS signal intensity is in inverse relation to the line width which is a direct measure of the exchange rate (Kanamori and Ross, 1997). These amide proton signals in MRS are unaffected by the NOE or short-T_2 species (e.g., in aliphatic compounds) that may interfere with increased S_{sat}/S_0 or decreased MTR_{asym} due to reduced proton exchange. The application of off-resonance irradiation for Z-spectra saturates a number of pH-irrelevant short-T_2 protons of lipids (6–16% of the brain *in vivo* in wet weight), proteins (~11%), and nucleic acids (~0.14%) *in vivo* (Clausen, 1969; Norton, 1975) along with the pH-relevant exchanging protons of Gln (<10 mM = ~0.02%) or other amides (~72 mM = ~0.14%) (Zhou et al., 2003). Given their high concentrations in brain *in vivo*, the unspecific saturation of irrelevant macromolecular protons and direct saturation of water protons may predominantly affect Z-spectra.

The present study also provides the first evidence about the influence of temperature on the *in vivo* brain MRS signals of exchangeable protons as well as on Z-spectrum and MTR_{asym}. The temperature-dependent Z-spectrum changes were shown to be similar in aliphatic and aromatic spectral ranges. Together with the observation of no significant difference in MTR_{asym} during hypercapnia, this symmetric change with temperature suggests that the R_1 of water protons is the dominant factor on Z-spectrum. A significantly greater temperature-dependent MTR change in the aromatic than in the aliphatic range, as seen in a simple water solution of Glc or barbituric acid *in vitro* (Ward et al., 2000; Zhou and van Zijl, 2006), would have indicated proton exchange as a contributing factor. However, this was not observed in brain *in vivo*, where a number of irrelevant protons are involved. In fact, MTR in brain *in vivo* was also shown to be significantly reduced by T_1-shortening of water protons induced by paramagnetic ions (Watanabe et al., 2010, 2016) similarly as by hypothermia in the present study. The contribution of T_2 in Z-spectra changes in the present study is supposed to be small compared to that of T_1 because (1) not T_2 but T_1 was shown to alter significantly with temperature, and (2) it is theoretically not straightforward to ascribe the changes in Z-spectra to changes in T_2 or T_2^* rather than to changes in water content, macromolecular content, and T_1.

Given the dominant availability of water protons in brain *in vivo* for a cross relaxation, it is not straightforward to ascribe the symmetric temperature-dependent Z-spectrum change to exchange-relayed NOE, i.e., NOE from aliphatic protons to exchanging protons rather than directly to water. Z-spectra from an aqueous solution of Glc or barbituric acid *in vitro* (Ward et al., 2000; Zhou and van Zijl, 2006) reveal a substantially greater temperature-dependent change in the aromatic rather than aliphatic range. This indicates that proton exchange rather than exchange-relayed NOE is the dominant factor. On the other hand, Z-spectrum from brain *in vivo* shows a symmetric change suggesting that neither proton exchange nor the exchange-relayed NOE is the dominant factor. This is because it is unlikely that (1) proton exchange is no longer dominant over exchange-relayed NOE if the Z-spectrum is obtained from brain *in vivo*, and (2) exchange-relayed NOE becomes so dominant as to cause a symmetric change: in order for this to occur, (a) all the exchanging protons contributing to Z-spectrum must be excited indirectly through NOE (from the aliphatic protons excited by an RF) as much as directly by an RF of the same power and (b) no NOE is allowed to occur between aliphatic and water protons. Both

(a) and (b) are very unlikely. Instead, the discrepancy between the *in vitro* asymmetric and *in vivo* symmetric changes can be explained as follows: (1) exchange-relayed NOE does not substantially contribute to Z-spectra in general, (2) proton exchange is the dominant factor in Z-spectra from aqueous solutions, and (3) R_1 is the dominant factor in Z-spectra from brain *in vivo*. Furthermore, if exchange-relayed NOEs were playing a role, i.e., the saturations were transferred between exchanging amide protons and aliphatic protons within Gln molecules, then the reduction in amide–water proton exchange during hypercapnia and/or hypothermia could have been observed by MRS as signal increases in the aliphatic protons of Gln as much as in their amide protons. A similar increase would then be expected for aliphatic proton signals of NAA, Glu, Glc, Cr, and PCr during hypothermia. However, none of these changes was observed as shown in Fig. 2a. There is no reason why intramolecular NOEs to the exchangeable protons must be assumed to be absent in these rapidly rotating molecules of intermediate size when intramolecular NOEs in other molecules were so strong as to cause a symmetric Z-spectrum change. Moreover, MTR in the aliphatic range rather increased during hypercapnia (Fig. 7a) in the present study, although a reduced exchange-relayed NOE would have reduced MTR. It still needs to be elucidated whether this MTR increase in the aliphatic range during hypercapnia is associated with the significant concentration increases of Cr and Glc.

The constantly negative MTR_{asym} is in line with previous reports (Hua et al., 2007; Desmond and Stanisz, 2012) and suggests that protons of aliphatic compounds are the dominant non-water protons in brain *in vivo*. The most prominent effect in the two Z-spectra shown here is the significantly greater saturation transfer from the protons in the aliphatic range than from those in the aromatic range, regardless of pH or temperature. This asymmetry results from the dipolar coupling between aliphatic protons and water protons. Compared to this obvious observation, the effects of reduced proton exchange on Z-spectra or MTR_{asym} are much smaller and not statistically significant. Therefore, we can conclude that dipolar coupling between aliphatic and water protons rather than proton exchange is the dominant factor in Z-spectra and MTR_{asym} of the brain *in vivo*. Accordingly, this work further demonstrates that irradiation at −3.5 ppm (H_2O) provides a much better white/gray matter contrast than at +3.5 ppm (H_2O), which may be exploited for structural and biochemical MRI studies of myelinated tissue. Irradiation at +3.5 ppm (H_2O) does provide white/gray contrast in agreement with recent reports (Jin et al., 2013; Dula et al., 2011), but much less than at −3.5 ppm (H_2O). This observation is in line with recent reports on MRS and CEST (Snoussi et al., 2015; Xu et al., 2015).

The observed changes of cerebral metabolite concentrations in response to isoflurane, hypercapnia, and hypothermia are in agreement with physiological mechanisms reported in the literature. Isoflurane impairs the cellular respiration (Rosenberg and Haugaard, 1973; Boretius et al., 2013) so that the lowered oxidative energy supply must be compensated for by enhanced anaerobic glycolysis generating Lac. A reduced pH by hypercapnia inhibits the anaerobic glycolysis (Yudkoff et al., 2000), which results in reduced Glc consumption, reduced Lac production, and compensatory utilization of Glu as metabolic fuel (Erecińska et al., 1988). In this truncated form of the tricarboxilic cycle bypassed by Glu utilization, CO_2 output would be reduced by 52% for ATP production in comparison to the intact cycle with Glc utilization (CO_2 production would be reduced by 67%, whereas that of ATP by only 31%) (Koolman and Röhm, 2003). Hypothermia reduces the overall energy consumption/demand, which leads to a proportional reduction of pyruvate and Lac. The changes in PCr and Cr can be used to estimate intracellular pH from the creatine phosphokinase equilibrium because neither the tissue concentration of ATP nor of ADP is significantly influenced by anesthesia, hypercapnia, or hypothermia (Folbergrová et al., 1972; Hägerdal et al., 1975; Nilsson and Siesjö, 1974; Siesjö et al., 1972). The concentration changes of these metabolites, which all carry

both exchangeable amide/hydroxyl protons and non-exchangeable protons, may have influenced the Z-spectrum changes or even cancelled the MTR_{asym} reduction caused by reduced amide–water proton exchange during hypercapnia.

The observed Glc concentration of 4.9 ± 1.0 mM in anesthetized mouse brain is in line with values of 4.3–6.1 mM reported for anesthetized rats at 22–37 °C (Nilsson and Siesjö, 1974; Hägerdal et al., 1975). A concentration difference from a normal human subject was ascribed to anesthesia because anesthetics generally increase the tissue Glc concentration as well as the tissue to blood Glc concentration ratio in brain *in vivo* (Nilsson and Siesjö, 1974).

Although *in vivo* MR data of experimental animals are most commonly acquired at 37 °C, normothermia is not a prerequisite for translational biomedical research. Experimental data in biochemistry, anatomy, histology, and pathology are often acquired *in vitro* or *ex vivo* at 20–25 °C or room temperature. In fact, proton MRS at low temperature may turn out to be advantageous in preclinical research as potential benefits comprise an increased signal-to-noise ratio (i.e., Boltzmann distribution), shorter T_1 relaxation times, and reduced proton exchange. Furthermore, hypothermia linearly reduces the minimum alveolar concentration for volatile anesthetics and even eliminates their need at 20 °C (Antognini, 1993). For anesthesia in humans, hypothermia has been used since centuries (Wong, 1983). So far, volatile anesthetics are most commonly used for *in vivo* MRS/MRI of animals because of their rapid induction, quick as well as pleasant recovery, and wide margin of safety. However, they alter the concentrations of most MRS-detectable cerebral metabolites (Boretius et al., 2013), which also holds true for other anesthetics (Choi et al., 2010; Hong et al., 2010; Boretius et al., 2013). In this regard, the present study shows a new perspective for metabolic MRS studies of animal brain *in vivo*.

There are abundant studies in the literature showing that amide or amine CEST signals are quite sensitive to a change of proton exchange (or pH) in diseases such as stroke. However, in these diseases, water and macromolecular content alter significantly. Temperature may change as well. While these factors predominantly affect the Z-spectrum, common CEST studies determine neither of them *in vivo*. Instead, they assume that these factors can be derived from the "conventional MT effect" and certain values obtained by MRI before subtracting their effect from Z-spectra to yield the "CEST effect." An arbitrary part of an experimental Z-spectrum is fitted to a certain model while the rest is excluded from fitting. Which part must be fitted to which model is still to be established and is so far commonly determined with regard to the resulting "CEST effect" map or "amide proton transfer" map: the method that created the map with the best contrast (or contrast-to-noise ratio) between healthy and pathological tissue is being employed. The derived values in the resulting maps *in vivo* commonly remain unverified: it is commonly not shown whether the data obtained *in vivo* really represent the true values *in vivo* (e.g., water and macromolecular content, amide proton concentration, proton exchange rate, or NOE) because these values *in vivo* are hardly obtainable. In fact, for proper quantification of the saturation transfer between multiple proton pools, quantification of each pool size is of essential importance. Furthermore, respective non-water protons must be kept fully and constantly saturated, while direct saturation of water protons must be completely avoided. None of these conditions can be fulfilled in a common CEST MRI investigation. As a result, despite the many studies claiming that CEST signals are sensitive to a change in pH-dependent amide–water proton exchange or in Cr concentration, none of them has ever pointed out that urea and Gln are involved in proton exchanges in brain *in vivo* or that PCr/Cr ratio correlates with pH *in vivo*, both of which are now demonstrated here by MRS. This further indicates that CEST MRI so far has been unable to separate the pH effect from the concentration effect.

As shown in the present study, it may be possible to detect a proton exchange effect in MRI of the brain *in vivo* but it is very small. Given that

amide–water proton exchange is more specifically observable by MRS, it needs to be elucidated whether CEST MRI indeed brings any additional diagnostic value to a conventional protocol combining (1) high-resolution T_1, T_2, diffusion, or magnetization transfer MRI for high sensitivity to changes in water/macromolecular content and (2) MRS for high specificity with respect to changes in pH, temperature, and metabolite concentrations.

In summary, the present work identifies the effects of pH and temperature on saturation transfer and proton exchange in MRS and MRI of mouse brain *in vivo*. Significant MRS changes in the amide proton signals of glutamine and other unspecific compounds are strongly correlated with each other and accompanied by concentration changes of creatine, phosphocreatine, glucose, lactate, and glutamate. MRI revealed that image contrast due to saturation transfer reflects reduced proton exchange and the distribution of aliphatic as well as aromatic/amide compounds.

Supplementary data to this article can be found online at http://dx.doi.org/10.1016/j.neuroimage.2016.03.013.

Conflict of interest

The authors declare that there is no conflict of interest including any financial, personal, or other relationships with other people or organizations.

References

Antognini, J.F., 1993. Hypothermia eliminates isoflurane requirements at 20 °C. Anesthesiology 78, 1152–1156.

Arús, C., Chang, Y.C., Barany, M., 1985. N-acetylaspartate as an intrinsic thermometer for ^{1}H NMR of brain slices. J. Magn. Reson. 63, 376–379.

Boretius, S., Tammer, R., Michaelis, T., Brockmöller, J., Frahm, J., 2013. Halogenated volatile anesthetics alter brain metabolism as revealed by proton magnetic resonance spectroscopy of mice in vivo. NeuroImage 69, 244–255.

Choi, C.B., Hong, S.T., Kim, S.Y., Woo, D.C., Choe, B.Y., Ryu, K.N., Kang, E.H., Yim, S.V., Lee, D.W., Pohmann, R., 2010. Differential neurochemical responses in the rat striatum with isoflurane or ketamine/xylazine anesthesia: in vivo proton MRS study at 16.4 T. Proc. Int. Soc. Magn. Reson. Med. 18, 2407.

Clausen, J., 1969. Gray-White Matter Differences. In: Lajtha, A. (Ed.), Handbook of NeurochemistryChemical Architecture of the Nervous System vol. 1. Plenum Press, New York, NY, pp. 273–300.

Cudalbu, C., Mlynárik, V., Xin, L., Gruetter, R., 2009. Comparison of T1 relaxation times of the neurochemical profile in rat brain at 9.4 tesla and 14.1 tesla. Magn. Reson. Med. 62, 862–867.

Desmond, K.L., Stanisz, G.J., 2012. Understanding quantitative pulsed CEST in the presence of MT. Magn. Reson. Med. 67, 979–990.

Duarte, J.M.N., Do, K.Q., Gruetter, R., 2014. Longitudinal neurochemical modifications in the aging mouse brain measured in vivo by ^{1}H magnetic resonance spectroscopy. Neurobiol. Aging 35, 1660–1668.

Dula, A.N., Asche, E.M., Landman, B.A., Welch, E.B., Pawate, S., Sriram, S., Gore, J.C., Smith, S.A., 2011. Development of chemical exchange saturation transfer at 7 T. Magn. Reson. Med. 66, 831–838.

Erecińska, M., Zaleska, M.M., Nissim, I., Nelson, D., Dagani, F., Yudkoff, M., 1988. Glucose and synaptosomal glutamate metabolism: studies with [^{15}N] glutamate. J. Neurochem. 51, 892–902.

Folbergrová, J., MacMillan, V., Siesjö, B.K., 1972. The effect of moderate and marked hypercapnia upon the energy state and upon the cytoplasmic NADH/NAD+ ratio of the rat brain. J. Neurochem. 19, 2497–2505.

Frahm, J., Michaelis, T., Merboldt, K.D., Bruhn, H., Gyngell, M.L., Hänicke, W., 1990. Improvements in localized proton NMR spectroscopy of human brain. Water suppression, short echo times, and 1 ml resolution. J. Magn. Reson. 90, 464–473.

Gruetter, R., 1993. Automatic, localized in vivo adjustment of all first-and second-order shim coils. Magn. Reson. Med. 29, 804–811.

Hägerdal, M., Harp, J., Siesjö, B.K., 1975. Effect of hypothermia upon organic phosphates, glycolytic metabolites, citric acid cycle intermediates and associated amino acids in rat cerebral cortex. J. Neurochem. 24, 743–748.

Haris, M., Nanga, R.P.R., Singh, A., Cai, K., Kogan, F., Hariharan, H., Reddy, R., 2012. Exchange rates of creatine kinase metabolites: feasibility of imaging creatine by chemical exchange saturation transfer MRI. NMR Biomed. 25, 1305–1309.

Hong, S.T., Choi, C.B., Pohmann, R., 2010. Measurement of the effects of different anesthetics in the rat thalamus by in vivo ^{1}H NMR spectroscopy at 16.4 T. Proc. Int. Soc. Magn. Reson. Med. 18, 2406.

Hua, J., Jones, C.K., Blakeley, J., Smith, S.A., van Zijl, P., Zhou, J., 2007. Quantitative description of the asymmetry in magnetization transfer effects around the water resonance in the human brain. Magn. Reson. Med. 58, 786–793.

Jin, T., Wang, P., Zong, X., Kim, S.G., 2013. MR imaging of the amide–proton transfer effect and the pH-insensitive nuclear overhauser effect at 9.4 T. Magn. Reson. Med. 69, 760–770.

Kanamori, K., Ross, B.D., 1997. Glial alkalinization detected in vivo by [1]H-^{15}N heteronuclear multiple-quantum coherence-transfer NMR in severely hyperammonemic rat. J. Neurochem. 68, 1209–1220.

Kass, I.S., Lipton, P., 1982. Mechanisms involved in irreversible anoxic damage to the in vitro rat hippocampal slice. J. Physiol. 332, 459–472.

Kazemi, H., Johnson, D.C., 1986. Regulation of cerebrospinal fluid acid–base balance. Physiol. Rev. 66, 953–1037.

Koolman, J., Röhm, K.H., 2003. Taschenatlas der Biochemie. third ed Georg Thieme, Stuttgart, Germany, pp. 136–147.

Moats, R.A., Lien, Y.H., Filippi, D., Ross, B.D., 1993. Decrease in cerebral inositols in rats and humans. Biochem. J. 15-18.

Mori, S., Eleff, S.M., Pilatus, U., Mori, N., van Zijl, P.C.M., 1998. Proton NMR spectroscopy of solvent-saturable resonances: a new approach to study pH effects in situ. Magn. Reson. Med. 40, 36–42.

Natt, O., Watanabe, T., Boretius, B., Frahm, J., Michaelis, T., 2003. Magnetization transfer MRI of mouse brain reveals areas of high neural density. Magn. Reson. Imaging 21, 1113–1120.

Nilsson, L., Siesjö, B.K., 1974. Influence of anaesthetics on the balance between production and utilization of energy in the brain. J. Neurochem. 23, 29–36.

Noda, L., Kuby, S.A., Lardy, H.A., 1954. Adenosine triphosphate-creatine transphosphorylase IV. Equilibrium studies. J. Biol. Chem. 210, 83–95.

Norton, W.T., 1975. Myelin: structure and biochemistry. In: Tower, D.B. (Ed.), The Nervous SystemThe Basic Neurosciences vol. 1. Raven Press, New York, pp. 467–481.

Ohlmeyer, P., 1946. Wärmemessung bei Fermentreaktionen. Z. Naturforsch. 1, 30–35.

Provencher, S.W., 1993. Estimation of metabolite concentrations from localized in vivo proton NMR spectra. Magn. Reson. Med. 30, 672–679.

Rosenberg, H., Haugaard, N., 1973. The effects of halothane on metabolism and calcium uptake in mitochondria of the rat liver and brain. Anesthesiology 39, 44–53.

Schulz, H., Johner, C., Eder, G., Ziesenis, A., Reitmeier, P., Heyder, J., Balling, R., 2002. Respiratory mechanics in mice: strain and sex specific differences. Acta Physiol. Scand. 174, 367–375.

Siesjö, B.K., Folbergrová, J., MacMillan, V., 1972. The effect of hypercapnia upon intracellular pH in the brain evaluated by the bicarbonate–carbonic acid method and from the creatine phosphokinase equilibrium. J. Neurochem. 19, 2483–2495.

Snoussi, K., Gillen, J.S., Horska, A., Puts, N.A., Pradhan, S., Edden, R.A., Barker, P.B., 2015. Comparison of brain gray and white matter macromolecule resonances at 3 and 7 Tesla. Magn. Reson. Med. 74, 607–613.

Tammer, R., Boretius, S., Michaelis, T., Pucher-Diehl, A., 2007. MRI compatible animal holder. European patent No. 2174154, US patent No. 8,334,698 B2.

Vermathen, P., Capizzano, A.A., Maudsley, A.A., 2000. Administration and ^{1}H MRS detection of histidine in human brain: application to in vivo pH measurement. Magn. Reson. Med. 43, 665–675.

Ward, K.M., Aletras, A.H., Balaban, R.S., 2000. A new class of contrast agents for MRI based on proton chemical exchange dependent saturation transfer (CEST). J. Magn. Reson. 143, 79–87.

Watanabe, T., Frahm, J., Michaelis, T., 2010. Myelin mapping in the living mouse brain using manganese-enhanced magnetization transfer MRI. NeuroImage 49, 1200–1204.

Watanabe, T., Frahm, J., Michaelis, T., 2016. In vivo brain MR imaging at subnanoliter resolution: contrast and histology. Magn. Reson. Med. Sci. 15, 11–25.

Watanabe, T., Frahm, J., Michaelis, T., 2012. Myelin mapping in the central nervous system of living mice using contrast-enhanced magnetization transfer MRI. NeuroImage 63, 812–817.

Watanabe, T., Radulovic, J., Spiess, J., Natt, O., Boretius, S., Frahm, J., Michaelis, T., 2004. In vivo 3D MRI staining of the mouse hippocampal system using intracerebral injection of MnCl2. NeuroImage 22, 860–867.

Whittingham, T.S., Lust, W.D., Christakis, D.A., Passonneau, J.V., 1984. Metabolic stability of hippocampal slice preparations during prolonged incubation. J. Neurochem. 43, 689–696.

Wong, K.C., 1983. Physiology and pharmacology of hypothermia. West. J. Med. 138, 227–232.

Xu, X., Yadav, N.N., Zeng, H., Jones, C.K., Zhou, J., van Zijl, P., Xu, J., 2015. Magnetization transfer contrast–suppressed imaging of amide proton transfer and relayed nuclear Overhauser enhancement chemical exchange saturation transfer effects in the human brain at 7 T. Magn. Reson. Med. http://dx.doi.org/10.1002/mrm.25990.

Yudkoff, M., Daikhin, Y., Nissim, I., Nissim, I., 2000. Acidosis and astrocyte amino acid metabolism. Neurochem. Int. 36, 329–339.

Zhou, J., van Zijl, P.C.M., 2006. Chemical exchange saturation transfer imaging and spectroscopy. Prog. Nucl. Magn. Reson. Spectrosc. 48, 109–136.

Zhou, J., Payen, J.F., Wilson, D.A., Traystman, R.J., van Zijl, P.C., 2003. Using the amide proton signals of intracellular proteins and peptides to detect pH effects in MRI. Nat. Med. 9, 1085–1090.